ChemPubSoc Europe

DOI: 10.1002/open.201900068

Open Access ChemistryOPEN Full Papers

Special Collection

Ammonothermal Synthesis, X-Ray and Time-of-Flight Neutron Crystal-Structure Determination, and Vibrational Properties of Barium Guanidinate, $Ba(CN_3H_4)_2$

Sebastian Benz,[a] Ronja Missong,[a] George Ogutu,[a] Ralf P. Stoffel,[a] Ulli Englert,[a] Shuki Torii,[d] Ping Miao,[d] Takashi Kamiyama,[d] and Richard Dronskowski*[a, b, c]

We report the crystal structure of $Ba(CN_3H_4)_2$ as synthesized from liquid ammonia. Structure solution based on X-ray diffraction data suffers from a severe pseudo-tetragonal problem due to extreme scattering contrast, so the true monoclinic symmetry is detectable only from neutron powder diffraction patterns, and structure solution and refinement was greatly aided by density-functional theory. The symmetry lowering is due to slight deviations of the guanidinate anion from the mirror plane in space group $P\bar{4}b2$, a necessity of hydrogen bonding. At 300 K, barium guanidinate crystallizes in $P2_1/c$ with $a = 6.26439(2)$ Å, $b = 16.58527(5)$ Å, $c = 6.25960(2)$ Å, and a monoclinic angle of $\beta = 90.000(1)°$. To improve the data-to-parameter ratio, anisotropic displacement parameters from first-principles theory were incorporated in the neutron refinement. Given the correct structural model, the positional parameters of the heavy atoms were also refinable from X-ray diffraction of a twinned crystal. The two independent guanidinate anions adopt the all-*trans*- and the *anti*-shape. The Ba cation is coordinated by eight imino nitrogens in a square antiprism with Ba–N contacts between 2.81 and 3.04 Å. The IR and Raman spectra of barium guanidinate were compared with DFT-calculated phonon spectra to identify the vibrational modes.

Introduction

Guanidine is one of the fundamental biomolecules and an important prototype for amino acids like arginine or creatine. Although guanidine was synthesized in 1861 by Strecker already,[1] its crystal structure remained unknown for almost one and a half centuries due to experimental problems in crystallization. Finally, the structure was determined by Yamada et al. in 2009[2] using single-crystal X-ray diffraction. In 2013 the entire structure including hydrogen positions and all anisotropic displacement parameters was re-refined based on single-crystal neutron-diffraction data.[3]

The strong base guanidine, its guanidinate salts of alkaline, alkaline-earth and also rare-earth metals and their structural chemistry have been a growing field of study within the recent years.[4–9] As guanidine is soluble in liquid ammonia, the synthesis of the guanidinates and growing single crystals can be achieved by dissolving a metal and guanidine under ammonothermal conditions. Within the crystal structure of $LiCN_3H_4$ and $NaCN_3H_4$, the $CN_3H_4^-$ molecular anion comprises an *anti*-conformation of the imino-hydrogen atoms, with both H-atoms pointing to different directions (see Figure 1). In contrast,

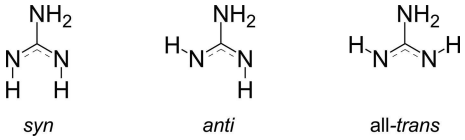

Figure 1. The possible conformations for the singly deprotonated guanidinate anion $CN_3H_4^-$. Reproduced from [8]. Copyright CC BY-NC-SA 4.0.

the structures of KCN_3H_4 and of the first rare-earth guanidinate, $Yb(CN_3H_4)_3$, contain these H-atoms pointing to the same direction (*syn*) but away from the amino-hydrogen atoms. In addition, the all-*trans* conformation was predicted for the structure of europium guanidinate.[9]

These examples reveal that the imino-hydrogen atoms show a distinct sensitivity towards the chemical environment and the packing of the structure-generating molecular anions; alternatively expressed, the imino-hydrogen orientation determines the efficiency of the crystal packing. In addition,

[a] Dr. S. Benz, Dr. R. Missong, G. Ogutu, Dr. R. P. Stoffel, Prof. Dr. U. Englert, Prof. Dr. R. Dronskowski
Chair of Solid-State and Quantum Chemistry, Institute of Inorganic Chemistry, RWTH Aachen University, Landoltweg 1, 52056 Aachen, Germany
E-mail: drons@HAL9000.ac.rwth-aachen.de
[b] Prof. Dr. R. Dronskowski
Jülich-Aachen Research Alliance, JARA-HPC, RWTH Aachen University, Aachen, Germany
[c] Prof. Dr. R. Dronskowski
Hoffmann Institute of Advanced Materials, Shenzhen Polytechnic, 7098 Liuxian Blvd, Nanshan District, Shenzhen, China
[d] Dr. S. Torii, Dr. P. Miao, Prof. Dr. T. Kamiyama
Institute of Materials Structure Science & J-PARC Center, High Energy Accelerator Research Organization (KEK), School of High Energy Accelerator Science, Sokendai, 203-1, Tokai-mura, Ibaraki 319-1106, Japan

Supporting information for this article is available on the WWW under https://doi.org/10.1002/open.201900068

Special Collection *An invited contribution to a Special Collection dedicated to Computational Chemistry***

guanidinates with bivalent metal cations such as $EuC(NH)_3$, $YbC(NH)_3$ and $SrC(NH)_3$ have been introduced containing a *doubly* deprotonated $C(NH)_3^{2-}$ unit, the nitrogen analogue of the carbonate anion.[7–9] In these salt-like solids, the anion adopts a trinacria motif, and then the amount of hydrogen bonding is insignificant. The chemistry and structural motifs have been recently reviewed.[10]

Here, we present an oxidation-controlled synthesis for preparing barium guanidinate, with the all new crystal structure solved from powder neutron diffraction and first-principles theory. It comprises the all-*trans*- and the *anti*-conformer within the same structure.

Results and Discussion

To synthesize phase-pure $Ba(CN_3H_4)_2$, exact stoichiometric amounts of reactants are vital. Furthermore, low concentration of the solvent NH_3 plays an important role. This ensures that no side products arise such as, for example, barium amide, $Ba(NH_2)_2$.

$Ba(CN_3H_4)_2$ can either be synthesized at room temperature or at higher temperatures (50 °C). In both cases, the product is crystalline. Synthesis at higher temperatures (50 °C) just reduces the reaction time to two days compared to five days for which the reaction is done at room temperature. This is because the reaction of the solvated electrons with ammonia is typically slow but can be accelerated by increasing the temperature. To grow crystals, however, it is recommended to carry out the reaction at room temperature and release the ammonia from the steel autoclaves very slowly.

In the first place, the neutron powder diffractograms were easily indexed in the tetragonal space group $P\bar{4}b2$ ($a = 6.266$ Å, $c = 16.58$ Å) because the metric is clearly tetragonal. Then, a raw structure model could be obtained by simulated annealing as implemented in the GSAS II program system. To do so, the CN_3-core of the guanidinate anion was used as a rigid body and placed on the two-fold rotation axis of the unit cell. As the refinement turned out to be unstable, the patterns were re-indexed and symmetry was reduced to the orthorhombic space group *Pcca*, despite showing the tetragonal metric. The additional degree of freedom allowed slight deviations of the CN_3-unit from the rotation axis in $P\bar{4}b2$ and resulted in an improved Rietveld fit of the diffraction pattern.

At this moment, DFT calculations turned out to be decisive. Initially the orthorhombic *Pcca* structure with intuitively positioned hydrogen atoms was used, followed by a structural optimization with VASP and also simulated lattice dynamics via Phonopy. The structural optimization led to a displacement of both amino hydrogen atoms from the CN_3 in-plane conformation. It then turned out that the proposed structure exhibited four bands with imaginary frequencies, each with the largest imaginary frequency found at Γ in the Brillouin zone (BZ); thus, the resulting eigenvectors could be easily applied to the smallest unit cell. If the maxima of the imaginary phonon bands had been somewhere else in the BZ, the simulation cell would have to be enlarged in order to fit to the wavelength of the imaginary mode.

The new structure was structurally optimized with VASP, once again, and it yielded a structure with space group *Pbcn* lower by ca. 27 kJ/mol than the initially optimized one, but it showed an even *stronger* displacement of the anion from the aforementioned two-fold rotational axis in the high-symmetry space group. Rietveld refinement gave a significant improvement in terms of pattern fitting and figure of merit.

Residuals in the scattering density map suggested a further reduction of space-group symmetry to the *translationengleich* subgroup $P2_1/b11$ ($P2_1/c$). Thus, the single guanidinate unit was split into two symmetry-independent ones, a structural consequence due to a hydrogen-bonding reason: this additional degree of freedom allowed the refinement of two guanidinates differing in shape, one adopting the all-*trans*- and the other the *anti*-conformation, eventually resulting in a dramatically improved fit quality. The lattice parameters converged to $a = 6.26439(2)$ Å, $b = 16.58527(5)$ Å, $c = 6.25960(2)$ Å and a monoclinic angle of $\beta = 90.000(1)°$.

Structural optimizations with subsequent phonon simulations based on the refined structure confirmed a lowered total energy by another 3 kJ/mol and no imaginary frequencies in the density of phonon states (DPS). That is to say that theory shows this structure to be a local minimum on the energy landscape; also, the occurrences of two guanidinate units was energetically preferable over an averaged structure with only the all-*trans*-conformation. Simply speaking, almost the entire structure matches the tetragonal crystal system but the packing necessity of a *single* hydrogen bond being part of one guanidinate anion requires monoclinic symmetry, without any consequences as regards the monoclinic angle which stays at 90.000(1)°. Even upon cooling down to 10 K, β does not deviate significantly and arrives at 89.9942(8)°, so the pseudosymmetry is kept at lowest temperature, too.

$Ba(CN_3H_4)_2$ crystallizes in the monoclinic space group $P2_1/c$ with four formula units per cell (Figure 2, left). All atoms occupy the general, low-symmetry 4*e* positions. The barium cation is eightfold coordinated by nitrogens atoms of the guanidinate anions, and this Ba^{2+} is located very close to the high-symmetry point $\bar{4}$ of the tetragonal space group $P\bar{4}b2$. The imino-nitrogen atoms form a distorted square antiprism in the distance range between 2.82–2.99 Å (Figure 2, right).

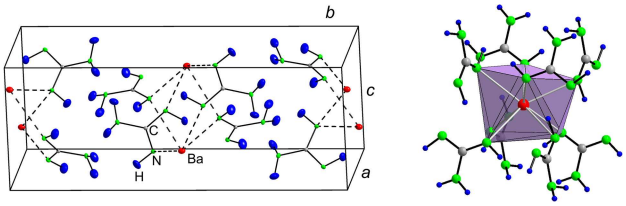

Figure 2. Left: Unit cell of the crystal structure of $Ba(CN_3H_4)_2$ at 10 K. Dashed lines highlight the Ba–N coordination, with carbon in grey, nitrogen in green, hydrogen in blue, and barium in red. Thermal ellipsoids are drawn at 50% probability (except Ba, probability: 98%). Right: Coordination polyhedron of barium cations. Imino-nitrogen atoms build up a slightly distorted square antiprism.

Formally, the structure is closely related to the $MoSi_2$ structure which was first described by *Nowotny* et al.[11] and crystallizes in the tetragonal space group *I*4/*mmm*, thereby higlighting the massive tetragonal pseudo-symmetry, also visible from the tetragonal metric. Figure 3 shows a comparison

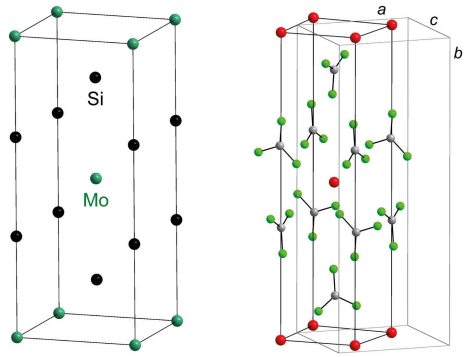

Figure 3. Comparison of the structure of $MoSi_2$ (Si: black, Mo: green) and the arrangement of Ba and CN_3H_4 within the structure of barium guanidinate. For a better view hydrogen atoms have been removed (barium in red, carbon in grey, nitrogen in green, and the unit cell light grey).

of the unit cell of $MoSi_2$ and the corresponding arrangement of the cation and the molecular anion within the structure of barium guanidinate.

If we concentrate on the H-bond distances between 2.32–2.54 Å, the guanidinate adopting the all-*trans*-conformation is surrounded by three guanidinate anions which coordinate the amino-NH_2 and one anion coordinating only one of the imino-NH groups. The *anti*-shaped guanidinate anion, however, is coordinated by three surrounding anions, two of them building H-bonds to the amino-NH_2 and one that binds via H-bonds to two imino-N atoms.

The extreme pseudo-symmetry in terms of the tetragonal system is obvious by looking at simulated X-ray reflection patterns as depicted in Figure 4 (left). For example, the *h*1*l* pattern exhibits only miniscule deviations from the ideal fourfold symmetry, which are usually masked by experimental uncertainties. The comparison with the simulated neutron-diffraction intensities (Figure 4, right) makes it clear, however, that the structure has a much lower symmetry than expected

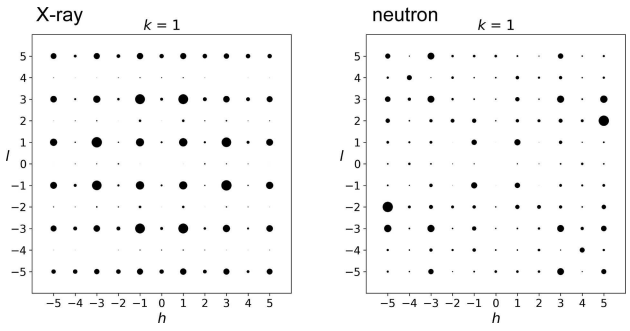

Figure 4. Simulated diffraction intensities of the *h*1*l* plane of $Ba(CN_3H_4)_2$ as based on X-ray (left) and neutron scattering factors (right).

from X-ray diffraction experiments, despite perfect tetragonal metric.

In addition, we attempted to solve and refine the structure based on XRD from a twinned crystal. The diffraction pattern could be indexed with a body-centered unit cell, a = 4.3974(8) Å, b = 4.3974(7) Å and c = 16.343(2) Å. An initial model was obtained in *I*4/*mmm*, the space group of the $MoSi_2$ parent structure. The fractional coordinates of the Ba cations and the central C atoms of the guanidinate anions are compatible with this tetragonal symmetry, but assignment of the N atoms required a descent in symmetry to the orthorhombic t_2 subgroup *Immm*. Refinement of the non-hydrogen atoms converged at favorable agreement factors (wR_2 = 0.0517, R = 0.0212 for 216 independent reflections and 19 variables); based on the X-ray intensities, no H atoms could be located, so it is impossible (taking into account the neutron information) to correctly catch the symmetry. With the barium cations placed at (0 0 0) and ($^1/_2$ $^1/_2$ $^1/_2$), all atoms of the guanidinate anions are situated on the mirror plane perpendicular to the crystallographic *a*-axis (see Figure 5).[12] The relationship of this unit cell

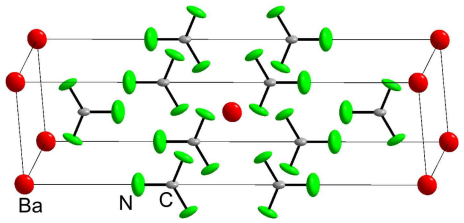

Figure 5. Unit cell of the crystal structure of $Ba(CN_3H_4)_2$ as refined from (twinned) single-crystal X-ray diffraction, showing carbon in grey, nitrogen in green, and barium in red. Thermal ellipsoids are drawn at 50% probability (except Ba, probability: 98%).

and the cell refined from neutron powder data becomes obvious when the cell is doubled via the diagonal of the *ab*-plane.

Eventually, the crystal structure was also refined based on neutron powder data collected at 10 K. Except for a reduction in volume, the structure at 10 K shows no significant differences to the structure measured at 300 K (see Table 2), as alluded to before (monoclinic angle).

As regards packing and volume chemistry, the molecular volume of $Ba(CN_3H_4)_2$ can be calculated as 98.12 $cm^3 mol^{-1}$. Substracting the Ba^{2+} increment[13] leaves 41.06 $cm^3 mol^{-1}$ for the $CN_3H_4^-$ unit. This volume is comparable to the doubly deprotonated $C(NH)_3^{2-}$ unit in $SrC(NH)_3$ (41.6 $cm^3 mol^{-1}$) and situated in the mid-range of hitherto studied guanidinates.

The assignment of vibrational bands (Table 1) was aided by the theoretically calculated eigenvectors of the respective phonon modes. Infrared (IR) transmittance and Raman spectroscopy of $Ba(CN_3H_4)_2$ reveal a complex spectrum (Figure 6) with an excellent agreement to the phonon calculations and just a slight shift to lower wavenumbers. Within the region between 3250 and 3500 cm^{-1} there are three groups of vibrations which are significantly broadened due to hydrogen bonding. The

Table 1. IR/Raman bands of $Ba(CN_3H_4)_2$ assigned using vibrations from DPS calculations.

Vibration	IR (cm^{-1})	Raman (cm^{-1})
$\nu(N–H_2)_{asym}$	3378	–
$\nu(N–H_2)_{sym}$, $\nu(N–H_{syn})$	3288	3290
$\nu(N–H_{anti})$	3212	3212
$\delta(N–H_2)_{sym}$	1560–1610	1550–1610
ν(C–N), δ(N–H)	1458	–
δ(N–H)	1319	–
δ(N–H)	1211	–
δ(N–H)	1180	1170
ν(C–N)	962	955 & 973
C-inversion by CN_3 plane	788	–
$\delta(CN_3)$ in plane	734	–
δ(C–N)	596	601
δ(C–N)	–	561
δ(C–N)	–	541

Table 2. Crystallographic data and refinement details for $Ba(CN_3H_4)_2$ at 10 K and 300 K.

Formula	$Ba(CN_3H_4)_2$	
Formula weight (g mol^{-1})	253.46	
Crystal system	monoclinic	
Space group	$P2_1/c$	
Temperature (K)	10 K	300 K
a (Å)	6.24146(2)	6.26440(2)
b (Å)	16.46439(4)	16.58527(5)
c (Å)	6.23913(2)	6.25960(2)
β (°)	89.9942(8)	90.000(1)
V ($Å^3$)	641.144(2)	650.351(2)
Z	4	
Cryst. density (gcm^{-3})	2.626	2.583
Radiation	neutron TOF	
No. reflections refined		
BS Bank	7803	2248
QA Bank	2276	1155
LA Bank	749	558
R_{F^2}, wR_p (%)		
BS Bank	20.181, 1.651	11.696, 1.280
QA Bank	6.740, 0.950	9.601, 0.915
LA Bank	7.588, 0.894	17.585, 1.034

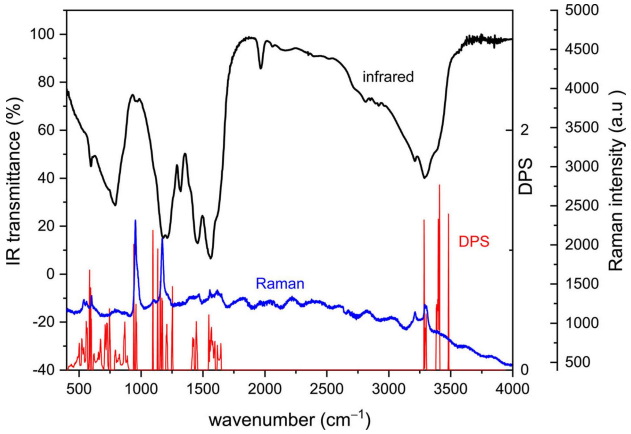

Figure 6. Infrared transmittance (black), Raman spectrum (blue) and calculated DPS (red) of barium guanidinate.

shoulder at 3378 cm^{-1} corresponds to the asymmetric $\nu(NH_2)$ vibration whereas the peak around 3288 cm^{-1} can be assigned to the symmetric NH/NH_2 stretching vibrations. Compared to that, the band at 3212 cm^{-1} is shifted to lower energies and resembles a stretching vibration of the *anti*-hydrogen atom pointing towards the imino-nitrogen atoms of the *syn*-guanidinate. Strong intermolecular hydrogen bonds are known to lead to a remarkable enhancement in absorption intensity and to the reduction in vibrational frequency.[14]

In the lower frequency region, bands between 596–962 cm^{-1} can be assigned to ν(C–N) and δ(C–N) vibrations. Bands between 1180–1319 cm^{-1} resemble δ(N–H) vibrations of imino-NH groups, and the peak at 1458 cm^{-1} was assigned to a combination of ν(C–N) and δ(N–H). The broad 1560–1610 cm^{-1} bands resemble symmetric deformation vibrations of the amino-NH_2 units of the all-*trans*- and the *anti*-guanidinate anion.

Conclusions

Barium guanidinate was synthesized and crystallized from elemental barium and guanidine in liquid ammonia. As the X-ray structure solution from pseudo-merohedrally twinned crystals turned out to be unsatisfactory and the scattering contrast of the atoms is extreme, we successfully performed a structure solution from neutron powder-diffraction patterns assisted by electronic-structure theory and theoretical phonon calculations. The structure suffers from massive pseudo-symmetry with a tetragonal metric and Ba atoms positioned very close to high-symmetry positions 2*c* and 2*b* in space group $P\bar{4}b2$. By leaving out the hydrogen atoms, the structure can still be described in the orthorhombic space group *Pbcn*. Symmetry reduction to the *translationengleich* subgroup $P2_1/c$ allows for sufficient degrees of freedom to handle two independent guanidinate anions of differing shape, as required for hydrogen bonding. Close relationship to the structure of $MoSi_2$ clarifies why single-crystal X-ray diffraction may mislead to the wrong space group *Immm* which resembles a *translationengleich* subgroup of index 2 of space group *I*4/*mmm*. The structure of barium guanidinate contains both conformers, the *syn*- and the *anti*-conformer within the unit cell, and the volume increment of the complex $CN_3H_4^-$ anion arrives at about 41.1 $cm^3\,mol^{-1}$.

The crystal structure as refined from neutron powder data was fully corroborated from theoretically calculated density of phonon states compared to experimental infrared and Raman spectra, and the calculations also allowed the assignment of vibrational modes to absorption bands or scattering peaks.

Experimental Section

Synthesis

CN_3H_5 was prepared in a one-pot synthesis by reacting guanidinium carbonate $(CN_3H_6)_2CO_3$ (Aldrich, 99%) with either sodium or potassium (Alfa, 99.95%) in a 1:1 molar ratio together with 15 cm^3 of solid, dried ammonia in a stainless-steel autoclave. After heating at 50 °C for five days, the autoclave was cooled to room temperature for one day, and then ammonia was released via a Schlenk line. A mixture of guanidine and alkali carbonate was recovered,

which was separated via sublimation for 7 days at 50 °C under vacuum to give colorless, phase-pure guanidine powder as a sublimate. Stoichiometric amounts of highly moisture-sensitive starting materials (elemental barium and guanidine) were weighed in the glovebox under argon to prevent contact with oxygen or moisture and then transferred into a steel autoclave. Barium was used as obtained from the manufacturer without any further purification. The reactants were evacuated for 15 minutes, and later 15 cm^3 of solid, dried ammonia was condensed (Linde, 99.999%, without further purification). The reaction was left to proceed for 5 days at room temperature. Ammonia was released in the Schlenk line via a mercury column, and the colorless powder was removed in the glove box.

Powder Diffraction

To obtain powder X-ray diffraction data of $Ba(CN_3H_4)_2$, a small amount of the white powder was filled in a 0.3 mm glass capillary and measured using a STOE STADI-P diffractometer at room temperature and Cu $K\alpha_1$ radiation in the 2θ range of 0–120° with step sizes of 0.010°. The powder pattern was indexed using DICVOL04 as provided in the WINXPOW suite.[15] Rietveld refinement was done using GSAS II.[16]

Neutron powder-diffraction patterns were recorded at the time-of-flight powder diffractometer SuperHRPD located at the Spallation Neutron Source at the Japan Proton Accelerator Research Complex (J-PARC).[17] Patterns were collected at 10 K (Figure 7) and 300 K using the backscattering bank with a resolution of $\Delta d/d = 0.03$–0.15% for 0.3–4.0 Å in *d*, the 90° bank with $\Delta d/d = 0.4$–0.7% for 0.4–7.5 Å in *d*, and the low-angle bank with $\Delta d/d = 0.7$-3.0% for 0.6–45 Å in *d*. The resulting powder diffractograms were indexed using the GSAS II program, and the neutron Rietveld refinements were performed with GSAS II as well. In the final step, unit cell parameters and atomic coordinates were simultaneously refined. Anisotropic displacement parameters were provided from first-principles theory such as to improve the overall accuracy, as successfully done before for related ureates[18] and detailed in more general terms.[19] Additional details concerning the structure determination are available in CIF format and have been deposited under the CCDC entry number 1890451–1890452. Copies of the data can be obtained free of charge from CCDC or from the supporting information.

Single-Crystal Diffraction

A small colorless platelet with approximate dimensions 0.02×0.01×0.01 mm^3 was mounted on a glass fiber and placed into the cold N_2 stream of the diffractometer. An Oxford Cryostream 700 instrument was used to maintain a data-collection temperature of 100 K. Intensity data were collected on a Bruker D8-Goniometer equipped with an APEX CCD detector. An Incoatec I-μS micro focus tube with focussing multilayer optics supplied MoKα radiation ($\lambda = 0.71073$ Å). 1886 intensities were measured in the ω-scan mode at room temperature and integrated with SAINT+.[20] SADABS[21] was used for scaling and absorption correction.

Spectroscopy and Theory

A Bruker ALPHA FT-IR-spectrometer placed in an argon-filled glove box and equipped with an ATR Platinum Diamond sample holder with a measurement range of 400–4000 cm^{-1} was employed to measure the infrared (IR) spectrum of $Ba(CN_3H_4)_2$. The results were compared with DFT-based phonon calculations, i.e., lattice vibrations that may or may not be infrared-active. By doing so, the specific vibrations of the measured bands were identified. Raman spectra were collected on a Horiba Labram Raman microscope with a measurement range of 100–4000 cm^{-1}.

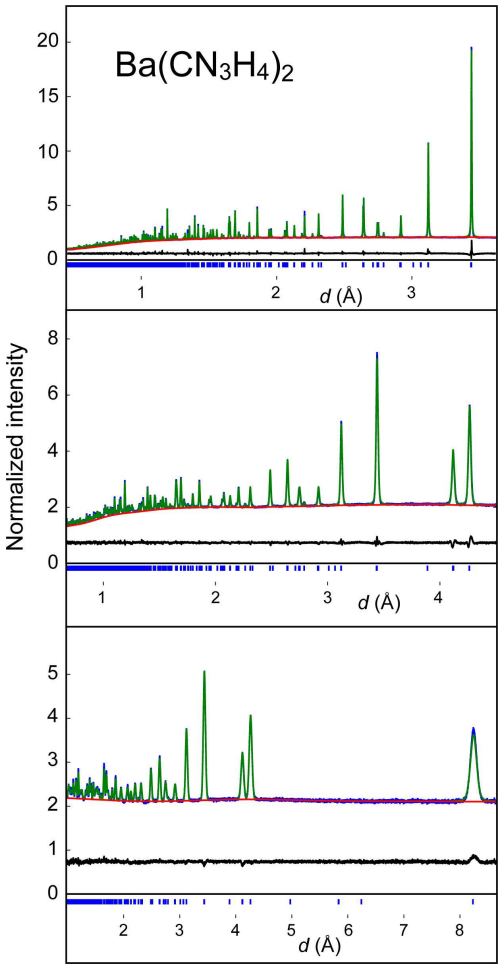

Figure 7. Rietveld refinement of the neutron powder diffraction patterns of $Ba(CN_3H_4)_2$ at 10 K showing the backscattering bank (top), the quarter angle bank (middle), and the low angle bank (bottom).

All DFT calculations were carried out using the *Vienna Ab initio Simulation Package* (VASP).[22] The PBE exchange-correlation functional[23] with the D3 dispersion-correction and Becke-Johnson damping[24] together with the projector augmented wave (PAW) method[25] was applied. For the electronic structure, a convergence criterion of at least 10^{-9} eV was used related to the respective simulation cell. Structural optimizations were carried out until the energetic difference between two iterative steps was well below 10^{-7} eV per simulation cell.

The phonon properties were derived using the *ab initio* force constant method as implemented in the Phonopy program[26] with forces resulting from VASP calculations on supercells with lattice vectors of at least 12 Å. Densities of phonon states (DPS)[27] and atomic displacement parameters (ADP) were calculated on dense meshes of reciprocal space points and checked for convergence.[19]

The densities of phonon states were checked for the appearance of imaginary phonon modes, which hint towards dynamical instability. If that was the case, new structures were modulated by applying the eigenvectors of the imaginary modes followed by structural optimizations using VASP.

Supplemental Information

Atomic positions (Table S1) and anisotropic atomic displacement parameters (Table S2) of $Ba(CN_3H_4)_2$ at 10 K, *Bärnighausen* trees (Figures S1 and S2) of $Ba(CN_3H_4)_2$ starting from the $MoSi_2$ archetype, and full crystallographic data in CIF format at 10 and 300 K.

Acknowledgements

The support by Deutsche Forschungsgemeinschaft is gratefully acknowledged. The DFT calculations were performed with computing resources thankfully granted by JARA-HPC from RWTH Aachen University under project JARA0033.

Conflict of Interest

The authors declare no conflict of interest.

Keywords: barium · X-ray diffraction · neutron diffraction · vibrational spectroscopy · density-functional theory

[1] A. Strecker, *Liebigs Ann. Chem.* **1861**, *118*, 151–177.
[2] T. Yamada, X. Liu, U. Englert, H. Yamane, R. Dronskowski, *Chem. Eur. J.* **2009**, *15*, 5651−5655.
[3] P. K. Sawinski, M. Meven, U. Englert, R. Dronskowski, *Cryst. Growth Des.* **2013**, *13*, 1730–1735.
[4] P. K. Sawinski, R. Dronskowski, *Inorg. Chem.* **2012**, *51*, 7425–7430.
[5] V. Hoepfner, R. Dronskowski, *Inorg. Chem.* **2011**, *50*, 3799–3803.
[6] P. K. Sawinski, V. L. Deringer, R. Dronskowski, *Dalton Trans.* **2013**, *42*, 15080–15087.
[7] R. Missong, J. George, A. Houben, M. Hoelzel, R. Dronskowski, *Angew. Chem. Int. Ed.* **2015**, *54*, 12171–12175; *Angew. Chem.* **2015**, *127*, 12339–12343.
[8] A. L. Görne, J. George, J. van Leusen, G. Dück, P. Jacobs, N. K. Chogondahalli, R. Dronskowski, *Inorg. Chem.* **2016**, *55*, 6161–6168.
[9] A. L. Görne, J. George, J. van Leusen, R. Dronskowski, *Inorganics* **2017**, *5*, 10.
[10] T. Scholz, A. L. Görne, R. Dronskowski, *Progr. Solid State Chem.* **2018**, *51*, 1–18.
[11] H. Nowotny, R. Kieffer, H. Schachner, *Monatsh. Chem.* **1952**, *83*, 1243–1252.
[12] R. Missong, *Synthese und Charakterisierung von Strontium- und Barium-guanidinat*, Dissertation, RWTH Aachen University, Aachen **2016**.
[13] W. Biltz, *Raumchemie der festen Stoffe*, Leopold Voss, Leipzig, **1934**.
[14] A. Mitsuzuka, A. Fujii, T. Ebata, N. Mikami, *J. Phys. Chem. A* **1998**, *102*, 9779–9784.
[15] WinXPow, *Powder Diffraction Software*, Stoe & Cie Ltd, Darmstadt, Germany, **1999**.
[16] H. Toby, R. B. von Dreele, *J. Appl. Crystallogr.* **2013**, *46*, 544−549.
[17] S. Torii, M. Yonemura, T. Y. Surya Panca Putra, J. Zhang, P. Miao, T. Muroya, R. Tomiyasu, T. Morishima, S. Sato, H. Sagehashi, Y. Noda, T. Kamiyama, *J. Phys. Soc. Jpn.* **2011**, *80*, SB020.
[18] K. B. Sterri, V. L. Deringer, A. Houben, P. Jacobs, C. M. N. Kumar, R. Dronskowski, *Z. Naturforsch. B* **2016**, *71*, 431–438.
[19] V. L. Deringer, J. George, R. Dronskowski, U. Englert, *Acc. Chem. Res.* **2017**, *50*, 1231–1239.
[20] SAINT+. Bruker AXS Inc., Madison, Wisconsin, USA, **2009**.
[21] SADABS. Bruker AXS Inc., Madison, Wisconsin, USA, **2008**.
[22] G. Kresse, J. Furthmüller, *Comput. Mater. Sci.* **1996**, *6*, 15–50.
[23] J. P. Perdew, K. Burke, M. Ernzerhof, *Phys. Rev. Lett.* **1996**, *77*, 3865.
[24] S. Grimme, J. Antony, S. Ehrlich, S. Krieg, *J. Chem. Phys.* **2010**, *132*, 154104; S. Grimme, S. Ehrlich, L. Goerigk, *J. Comput. Chem.* **2011**, *32*,1456.
[25] P. E. Blöchl, *Phys. Rev. B* **1994**, *50*, 17953–17979.
[26] A. Togo, I. Tanaka, *Scripta Mater.* **2015**, *108*, 1–5.
[27] R. P. Stoffel, C. Wessel, M.-W. Lumey, R. Dronskowski, *Angew. Chem. Int. Ed.* **2010**, *49*, 5242–5266; *Angew. Chem.* **2010**, *122*, 5370–5395.

Manuscript received: February 22, 2019